LAWRENCE
LIVERMORE
NATIONAL
LABORATORY

Papillary muscles contraction does not change ventricular wall mechanics

V. Gurev, J. Korte, O. Hafez, J. L. Fattebert, D. F. Richards, J. J. Rice

August 31, 2015

Disclaimer

This document was prepared as an account of work sponsored by an agency of the United States government. Neither the United States government nor Lawrence Livermore National Security, LLC, nor any of their employees makes any warranty, expressed or implied, or assumes any legal liability or responsibility for the accuracy, completeness, or usefulness of any information, apparatus, product, or process disclosed, or represents that its use would not infringe privately owned rights. Reference herein to any specific commercial product, process, or service by trade name, trademark, manufacturer, or otherwise does not necessarily constitute or imply its endorsement, recommendation, or favoring by the United States government or Lawrence Livermore National Security, LLC. The views and opinions of authors expressed herein do not necessarily state or reflect those of the United States government or Lawrence Livermore National Security, LLC, and shall not be used for advertising or product endorsement purposes.

Papillary muscles contraction does not change ventricular wall mechanics

Viatcheslav Gurev[1], James Korte[1], Omar Hafez[3], Jean-Luc Fattebert[2], David F. Richards[2],
John J Rice[1]

[1] IBM Research, Yorktown Heights, USA
[2] Lawrence Livermore National Laboratory, Livermore, USA
[3] UC Davis, Davis, USA

Abstract

Papillary muscles play a crucial role to support valves in the ventricles. However, much less is known about the role in ventricular wall mechanics. Evidence in the literature is inconclusive, showing both of changes in wall strain and indications of no changes in strain after detachment of papillary muscles. We designed a high-resolution 3D model of canine ventricles to investigate the effects of papillary muscles on strain in the regions overlying papillary muscles. An anatomical model was obtained from in-vitro MRI and a realistic fiber geometry assuming transmural rotation in the ventricular wall. Boundary conditions were either: 1) the attached state in which movements of the papillary muscle tips were restricted to the plane parallel to the base of the ventricles; or 2) the detached state where no constraints were placed on the muscle tips. Strains were measured at locations overlying anterior papillary muscle and compared between attached and detached papillary muscle states. In simulation of typical physiological contractions, we found essentially identical pattern in all strain components in the two cases with minor changes near the anterior papillary muscle. Further studies will be required to generalize the results to more anatomical reconstructions and a wider range of conditions.

1.   Introduction

Replacement of the mitral valve is a common procedure to prevent mitral regurgitation. This procedure makes the function of chordae tendineae unnecessary. Yet, multiple patient followup studies demonstrate that preservation of chordae tendineae is important for normal heart function even after mitral valve replacement (for full review see [1]). However, why chordal transection (CT) negatively affects cardiac function and outcome is unclear. A leading hypothesis is that contraction of papillary muscle (PM) are required to provide normal contraction of the wall overlying PM. Therefore, several studies investigated strain in the regions overlying PM and compared with distant regions of the free wall using canine and sheep animal models [2–4]. Other experiments compared wall mechanics before and after CT [5]. These experimental models have shown significant difference between strain in tissue overlying PM and free wall, although some authors concluded that this difference may not be related to the presence of PM but instead due to some other regional differences in ventricular contraction [3]. In any case, experimental models are still unable to explain why preservation of chordae tendineae is important for better mitral replacement surgery outcomes.

Experimental models have several significant shortcomings. First, the number of locations for strain monitoring is limited. Results in animal models are difficult to translate to human ventricles as the morphology of PM could be different for canine or sheep ventricles compared to human [6]. Finally, multiple factors such as ischemia near PM or other abnormalities are difficult to take in account in experimental settings.

The goal of this paper is to resolve some experimental inconsistencies and to characterize the strain in the regions overlying PM in the canine ventricles. Recently, we developed a computational model of ventricular mechanics that allows for simulation of ventricular contraction with higher spatial resolution than previously possible [7]. We are able to use finite element meshes that represent the complex ventricular geometry of endocardial surface of the ventricles with PM and trabeculation. The newly developed model is ideal to investigate the strain in ventricular wall and the effect of PM on wall deformations. This study is a logical first step by simulating ventricular mechanics with and without PM before transitioning to more sophisticated models of human ventricles.

2.   Methods

2.1.   Computational model

Full details on the methods for the computational model of the ventricles can be found elsewhere [7]. Here, we de-
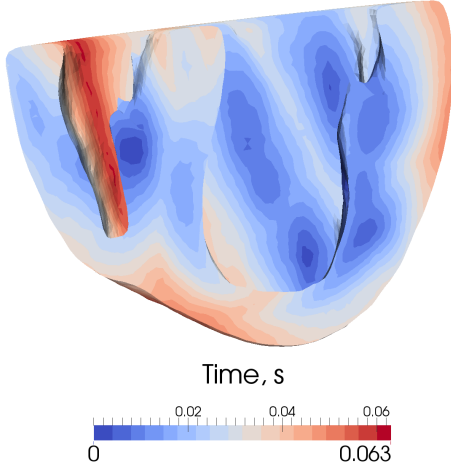
Figure 1. Time of electrical activation of the heart.

scribe only changes that we introduce for this particular study. The model comprises three main components: 1) a 3D finite element model of cardiac contraction which is based on an accurate canine ventricular geometry reconstructed from publicly available datasets [8]; 2) a muscle contraction model [9]; and 3) a circulatory model using CircAdapt [9].

2.2. Finite element model

The finite element mesh is composed of 313,802 tetrahedral finite elements, we used P1-P1 tetrahedral linear elements with stabilization [10]. Here, the parameter δ from [10] was chosen based on a set of simulations to match strain between simulations of ventricular contraction made with P2-P1 and P1-P1 elements.

As usual, $\Omega_0 \subset \mathbb{R}^3$ and $\Omega \subset \mathbb{R}^3$ represent the cardiac tissue in undeformed and deformed configurations. For $\mathbf{X} \in \mathbf{\Omega_0}$, $\mathbf{x(X)} \in \mathbf{\Omega}$ is the corresponding point in Ω. The deformation gradient F and right Cauchy-Green deformation tensor C are defined by $F = \frac{\partial \mathbf{x}}{\partial \mathbf{X}}$ and $C = F^{\mathrm{T}} F$. As in the previous paper [7], we use an exponential constitutive law converted to nearly incompressible formulation:

$$W(C) = \frac{C_1}{2} \left(e^Q - 1 \right), \quad (1)$$

$$\begin{aligned} Q = & \quad b_{ff} E_{ff}^2 + b_{ss} E_{ss}^2 + b_{nn} E_{nn}^2 \\ & + b_{fs}(E_{fs}^2 + E_{sf}^2) + b_{fn}(E_{fn}^2 + E_{nf}^2) \\ & + b_{ns}(E_{ns}^2 + E_{sn}^2), \quad (2) \end{aligned}$$

where $E = \frac{1}{2}(C - I)$.

2.3. Mechanical boundary conditions

Mechanical boundary conditions are similar to those in our previous simulations [7]. However, we added additional boundary conditions for anterior and posterior PM: the tips of PM are allowed to move only in the plane parallel to the base of the ventricles. To demonstrate the effects of PM attachment, we employ two sets of boundary conditions, one with restricted movement of the tips and one without restriction.

2.4. Simulation protocol

Electrical activation was simulated using the solver Cardioid [11]. We chose to simultaneously stimulate several points inside PM and points near the endocardial surface at the apex and the base of the ventricles to simulate typical activation in large mammalian hearts [12,13]. Figure 1 shows electrical activation in a cut of the ventricles through the anterior PM with a view on posterior wall. The steady state of the CircAdapt model requires long pacing that is computationally inefficient to perform on a high-resolution model. Therefore, we used a coarser finite element mesh of the same shape and simulated approximately 50 cardiac beats. At the end, state variables of the circulatory model were saved and reused in the high-resolution model.

2.5. Model parameters

Parameters of the model are given in the Table 1.
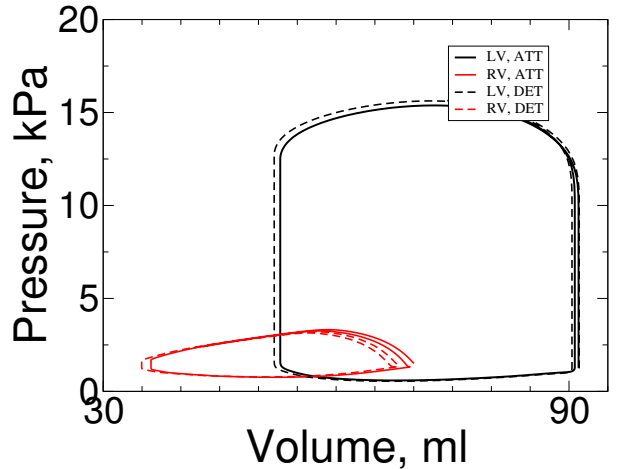
2.6. Strain calculation

Figure 2. Pressure-volume loop for two sets of boundary conditions.

Strain was calculated midway between the apex and base. To define a local coordinate system and to place

Table 1. Parameters of the model

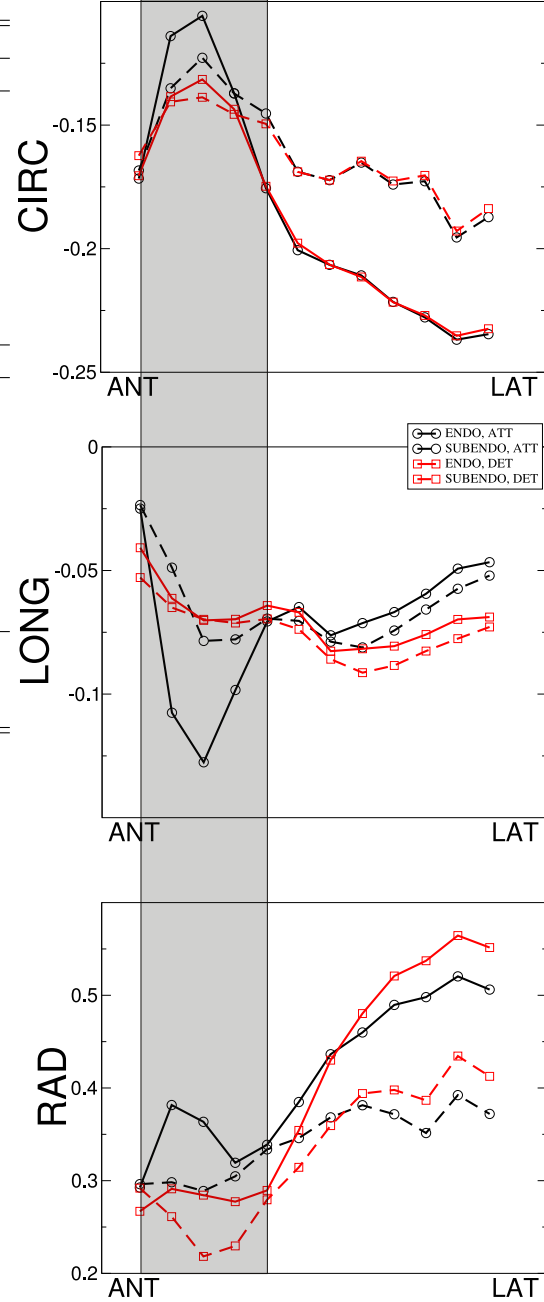| Parameter	Value	Units
Muscle model		
C_{rest}	0	-
L_{sc0}	1.51	μm
$L_{se,iso}$	0.04	μm
τ_D	33.8	ms
τ_R	28.1	ms
τ_{sc}	292.5	ms
σ_{act}	70	kPa
Cardiac cycle time	600	ms
Finite element model		
C_1	0.88	kPa
b_{ff}	8.0	-
b_{ss}	6.0	-
b_{nn}	3.0	-
b_{fs}	12.0	-
b_{fn}	3.0	-
b_{ns}	3.0	-
Circulatory model		
Mean systemic blood flow	46	$mL\ s^{-1}$
Mean systemic arterial blood pressure	10	kPa
Mean pulmonary arteriovenous pressure drop	0.5	kPa

Figure 3. Peaks of end-systolic finite strains with respect to end-diastole. Locations are taken circumferentially from the beginning of the region overlying anterior PM (ANT) to the lateral wall (LAT). Gray area shows the span of the region overlying the anterior PM. Two transmural points (endocardium - solid lines and subendocardum - dashed lines) are shown.

the points where the strains were calculated, we solved the Poisson equation $\nabla^2\phi(x) = 0$ on the finite element mesh with Dirichlet boundary condition on the endocardial and epicardial surfaces of the left (LV) and right (RV) ventricles. Values of ϕ were set to $\phi = 0$ at the endocardial surface of the LV and $\phi = 1$ on the endocardial surface of the RV and epicardium of the ventricles. Such boundary conditions produced a scalar field ϕ with gradient $\nabla\phi$ directed from the endocardium to the epicardium of the LV. We derived three iso-surfaces with $\phi = 0.1$, $\phi = 0.5$ and $\phi = 0.9$ for endocardium, midwall and epicaridum. For a given location on the midwall ($\phi = 0.5$), five points were chosen on a transmural line segment. We first selected the point p_m at the midwall iso-surface and found the gradient $\vec{r} = \nabla\phi(p_m)$. There were 12 of such selected points, ranging from the area under the papillary muscle to the lateral wall (Fig. 3). This gradient was defined to be the radial direction and used to construct the line $x = p_m + \alpha\vec{t}$. Next we found intersections p_{endo} and p_{epi} of this line with endocardial and epicardial iso-surfaces. All strains for a single location were calculated transmurally on a segment between p_{endo} and p_{epi}. We obtained the circumferential direction $\vec{c} = \frac{\vec{t} \times \vec{z}}{\|\vec{t} \times \vec{z}\|}$, where $\vec{z} = (1, 0, 0)$ was the normal vector to the plane of ventricular base. The longitudinal direction was $\vec{l} = \vec{c} \times \vec{r}$.

3. Results and Discussion

Pressure-volume loops for the LV and RV for boundary conditions with attached and detached PM are shown

in Figure 2. Our findings are consistent with an increase of ventricular compliance due to CT; however, the differences between two boundary conditions are very small, resulting in only a few milliliters of LV volume increase (see Figure 2). Unlike in previous experiments, we observed a slight increase in systolic pressure and increased stroke volume.

Figure 3 shows the peaks of systolic strains at several locations taken circumferentially at the midway between base and apex. Strain locations begin at anterior wall, where the region overlying anterior PM starts, spanning through lateral wall and ending near the region overlying posterior PM. Gray areas label the region overlying the anterior PM. We show only two points near endocardium from the five evenly distributed transmural points for every location because the others showed minor differences. This graph agrees with previous experimental findings [2] demonstrating reduced wall thickening in the region. In our results, radial and circumferential strain magnitudes are reduced overlying PM. However, when PM are attached, the magnitude of longitudinal strain in the region overlying PM is increased, probably a result of longitudinally oriented fibers in PM pulling on the tissue. Muscle detachment only affects strain in a very small region at endocardium overlying PM.

4. Conclusions

Our simulations showed only small and localized effects of strain produced by PM. Therefore, the study suggests little deterioration of ventricular contraction after CT. As such, the study does not suggest a mechanism for the worse outcome after mitral valve replacement with CT. However, other conditions related to mitral valve replacement such as ischemic mitral regurgitation could play a role. Also, the effects of CT on wall mechanics could be larger in human hearts, so we will rerun simulations with a computational model of human ventricles in later studies.

Acknowledgements

References

[1] Solomon N, Pranav S, Naik D, Sukumaran S. Importance of preservation of chordal apparatus in mitral valve replacement. Expert review of cardiovascular therapy 2006; 4(2):253–261.

[2] Holmes JW, Takayama Y, LeGrice I, Covell JW. Depressed regional deformation near anterior papillary muscle. American Journal of Physiology Heart and Circulatory Physiology 1995;269(1):H262–H270.

[3] Itoh A, Stephens EH, Ennis DB, Carlhall CJ, Bothe W, Nguyen TC, Swanson JC, Miller DC, Ingels NB. Contribution of myocardium overlying the anterolateral papillary muscle to left ventricular deformation. American Journal of Physiology Heart and Circulatory Physiology 2012; 302(1):H180–H187.

[4] Miyoshi H, Takayama Y, Tamura T, Kitashiro S, Izuoka T, Saito D, Imuro Y, Iwasaka T. Regional myocardial function at the papillary muscle insertion site. The Japanese journal of physiology 2001;51(1):109–114.

[5] Takayama Y, Holmes JW, LeGrice I, Covell JW. Enhanced regional deformation at the anterior papillary muscle insertion site after chordal transsection. Circulation 1996; 93(3):585–593.

[6] Axel L. Papillary muscles do not attach directly to the solid heart wall. Circulation 2004;109(25):3145–3148.

[7] Gurev V, Pathmanathan P, Fattebert JL, Wen HF, Magerlein J, Gray RA, Richards DF, Rice JJ. A high-resolution computational model of the deforming human heart. Biomechanics and Modeling in Mechanobiology January 2015; 1–21. ISSN 1617-7959, 1617-7940.

[8] Helm PA, Younes L, Beg MF, Ennis DB, Leclercq C, Faris OP, McVeigh E, Kass D, Miller MI, Winslow RL. Evidence of structural remodeling in the dyssynchronous failing heart. Circulation Research 2006;98(1):125–132.

[9] Lumens J, Delhaas T, Kirn B, Arts T. Three-wall segment (triseg) model describing mechanics and hemodynamics of ventricular interaction. Annals of biomedical engineering 2009;37(11):2234–2255.

[10] Klaas O, Maniatty A, Shephard MS. A stabilized mixed finite element method for finite elasticity: Formulation for linear displacement and pressure interpolation. Computer Methods in Applied Mechanics and Engineering 1999; 180(1):65–79.

[11] Richards DF, Glosli JN, Draeger EW, Mirin AA, Chan B, Fattebert JL, Krauss WD, Oppelstrup T, Butler CJ, Gunnels JA, et al. Towards real-time simulation of cardiac electrophysiology in a human heart at high resolution. Computer methods in biomechanics and biomedical engineering 2013;16(7):802–805.

[12] Spach MS, Barr RC. Ventricular intramural and epicardial potential distributions during ventricular activation and repolarization in the intact dog. Circulation research 1975; 37(2):243–257.

[13] Durrer D, Van Dam RT, Freud G, Janse M, Meijler F, Arzbaecher R. Total excitation of the isolated human heart. Circulation 1970;41(6):899–912.

Address for correspondence:

Viatcheslav Gurev
IBM Research Thomas J. Watson Research Center, 1101 Kitchawan Rd, Yorktown Heights, NY 10598
vgurev@us.ibm.com